Production of dileptons via photon-photon fusion in proton-proton collisions with one forward proton measurement

A. Szczurek[1,2], B. Linek and M. Luszczak

[1] The Henryk Niewodniczański Institute of Nuclear Physics Polish Academy of Sciences [2]University of Rzeszów

EPS-HEPP, Hamburg, July 26 2021

Contents

- Introduction
- Sketch of the formalism
- Inclusive production
  (integrated cross section, distributions, structure functions, ...)
- Cut on ξ variable(s)
  (integrated cross section, distributions, structure functions, ...)
- Range of x_{Bj} and/or Q^2 tested in the $pp \to l^+ l^- (p)$ processes
- (Mini)jet or final state emissions
- *SuperChic* results
  (distributions, differential gap survival factor)
- Conclusions and outlook

Introduction

- We wish to discuss production of dilepton pairs in proton-proton collisions via photon-photon fusion including photon transverse momenta.
- Both ATLAS and CMS performed relevant measurements (without and with proton measurements)
- Here we concentrate on the case with one forward proton (CMS (poor statistics), ATLAS (better statistics, 14.6 fb^{-1}, both e^+e^- and $\mu^+\mu^-$). A. Szczurek, B. Linek and M. Luszczak, arXiv:2107.02535.
- Our group was the first which proposed to use the formalism with photon transverse momenta.
- The same formalism can be also used for production of W^+W^- and $t\bar{t}$ pairs.
- Here we wish to discuss consequences of proton measurement for the cross section, differential distributions, gap survival factor, etc.
- We will also use the popular SuperChic-4 generator where the same formalism was implemented. It also includes kinemtics-dependent soft gap survival factor as developed by the Durham group.

Our previous papers on the subject

- G.G. da Silveira, L. Forthomme, K. Piotrzkowski, W. Schäfer and A. Szczurek, Ćentral $\mu^+\mu^-$ production via photon-photon fusion in proton-proton collisions with proton dissociation", JHEP **02** (2015) 159.
- M. Luszczak, W. Schäfer and A. Szczurek, "Two-photon dilepton production in proton-proton collisions: Two alternative approaches", Phys. Rev. **D93** (2016) 074018.
- M. Luszczak, W. Schäfer and A. Szczurek, "Production of W^+W^- pairs via $\gamma^*\gamma^* \to W^+W^-$ subprocess with photon transverse momenta", JHEP**05** (2018) 064.
- P. Lebiedowicz and A. Szczurek, "Exclusive and semiexclusive production of $\mu^+\mu^-$ pairs with Delta isobars and other resonances in the final state and the size of absorption effects", Phys. Rev. **D98** (2018) 053007.
- L. Forthomme, M. Luszczak, W. Schäfer and A. Szczurek, "Rapidity gap survival factors caused by remnant fragmentation for W^+W^- pair production via $\gamma^*\gamma^* \to W^+W^-$ subprocess with photon transverse momenta", Phys. Lett. **B789** (2019) 300.
- M. Luszczak, L. Forthomme, W. Schäfer and A. Szczurek, "Production of $t\bar{t}$ pairs via $\gamma\gamma$ fusion with photon transverse momenta and proton dissociation", JHEP **02** (2019) 100.

The mechanisms considered

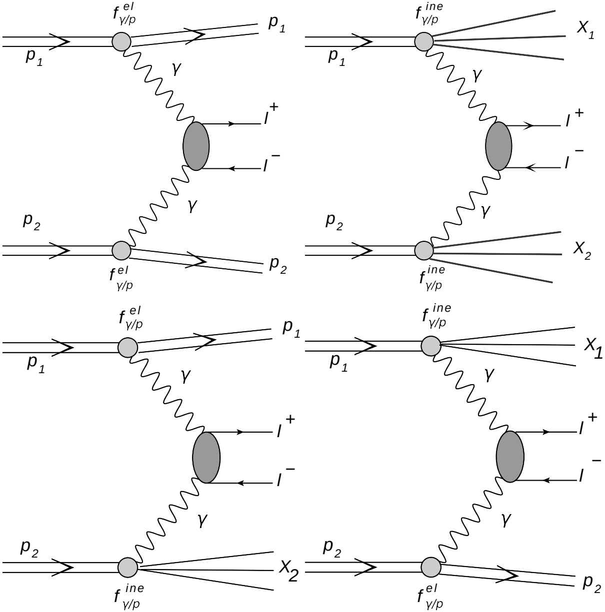

Resonance production

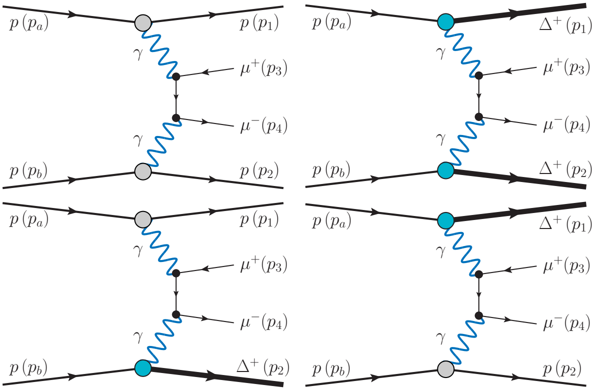

Rysunek: Four different categories of $\gamma\gamma$ fusion mechanisms of dilepton production in proton-proton collisions with resonances in the final state.

Sketch of the formalism

In the k_T-factorization approach, the cross section for $l^+ l^-$ production can be written in the form

$$\frac{d\sigma^{(i,j)}}{dy_1 dy_2 d^2\boldsymbol{p}_1 d^2\boldsymbol{p}_2} = \int \frac{d^2\boldsymbol{q}_1}{\pi \boldsymbol{q}_1^2} \frac{d^2\boldsymbol{q}_2}{\pi \boldsymbol{q}_2^2} \mathcal{F}^{(i)}_{\gamma^*/A}(x_1, \boldsymbol{q}_1)\, \mathcal{F}^{(j)}_{\gamma^*/B}(x_2, \boldsymbol{q}_2) \frac{d\sigma^*_{\gamma^*\gamma^* \to l^+l^-}(p_1, p_2; \boldsymbol{q}_1, \boldsymbol{q}_2)}{dy_1 dy_2 d^2\boldsymbol{p}_1 d^2\boldsymbol{p}_2}, \tag{1}$$

where the indices $i, j \in \{\mathrm{el}, \mathrm{in}\}$ denote elastic or inelastic final states.

Here the photon flux for inelatic case is integrated over the mass of the remnant.

Sketch of the formalism

The longitudinal momentum fractions of photons are obtained from the rapidities and transverse momenta of final state l^+l^- as:

$$
\begin{aligned}
x_1 &= \sqrt{\frac{\boldsymbol{p}_1^2 + m_l^2}{s}} e^{+y_1} + \sqrt{\frac{\boldsymbol{p}_2^2 + m_l^2}{s}} e^{+y_2} \, , \\
x_2 &= \sqrt{\frac{\boldsymbol{p}_1^2 + m_l^2}{s}} e^{-y_1} + \sqrt{\frac{\boldsymbol{p}_2^2 + m_l^2}{s}} e^{-y_2} \, .
\end{aligned} \tag{2}
$$

Four-momenta of intermediate photons:

$$
\begin{aligned}
q_1 &\approx \left(x_1 \frac{\sqrt{s}}{2}, \vec{q}_{1t}, x_1 \frac{\sqrt{s}}{2} \right) \, , \\
q_2 &\approx \left(x_2 \frac{\sqrt{s}}{2}, \vec{q}_{2t}, -x_2 \frac{\sqrt{s}}{2} \right) \, .
\end{aligned} \tag{3}
$$

Photon fluxes

The integrated fluxes for elastic and inelastic processes can be found in our published papers (see also Budneev, Ginzburg, Serbo et al.)

- The elastic flux is expressed via proton electromagnetic form factors.
- The inelastic flux is expressed via proton structure function (F_2 and F_L).

If one is interested in modeling what happens with the proton remnant than the formalism must be extended. Then the unintegrated inelastic photon distribution (flux) can be written as:

$$\mathcal{F}_{ine}(x, q_t^2) = \int dM^2 \frac{d\mathcal{F}_{ine}}{dM^2}(x, q_t^2, M^2) \; , \tag{4}$$

where $\frac{d\mathcal{F}_{ine}}{dM^2}(x, q_t^2, M^2)$ is a more differential photon distribution in the proton. We shall call it *doubly-unintegrated* photon distribution (flux).

The latter distribution was used to calculate differential distributions for production of W^+W^- (FLSS2019) or $t\bar{t}$ (LFSS2019) pairs with rapidity gap at midrapidities.

Photon fluxes

Inelastic flux:

$$\begin{aligned}\mathcal{F}^{\rm in}_{\gamma^* \leftarrow A}(z, \boldsymbol{q}) &= \frac{\alpha_{\rm em}}{\pi} \Big\{ (1-z) \Big(\frac{\boldsymbol{q}^2}{\boldsymbol{q}^2 + z(M_X^2 - m_p^2) + z^2 m_p^2} \Big)^2 \frac{F_2(x_{\rm Bj}, Q^2)}{Q^2 + M_X^2 - m_p^2} \\ &+ \frac{z^2}{4 x_{\rm Bj}^2} \frac{\boldsymbol{q}^2}{\boldsymbol{q}^2 + z(M_X^2 - m_p^2) + z^2 m_p^2} \frac{2 x_{\rm Bj} F_1(x_{\rm Bj}, Q^2)}{Q^2 + M_X^2 - m_p^2} \Big\}, \end{aligned} \tag{5}$$

Ingredients: F_1 and F_2 structure functions

Elastic flux:

$$\begin{aligned}\mathcal{F}^{\rm el}_{\gamma^* \leftarrow A}(z, \boldsymbol{q}) &= \frac{}{\pi} \Big\{ (1-z) \Big(\frac{\boldsymbol{q}^2}{\boldsymbol{q}^2 + z(M_X^2 - m_p^2) + z^2 m_p^2} \Big)^2 \frac{4 m_p^2 G_E^2(Q^2) + Q^2 G_M^2(Q^2)}{4 m_p^2 + Q^2} \\ &+ \frac{z^2}{4} \frac{\boldsymbol{q}^2}{\boldsymbol{q}^2 + z(M_X^2 - m_p^2) + z^2 m_p^2} G_M^2(Q^2) \Big\}. \end{aligned} \tag{6}$$

Ingredients: Electromagnetic form factors

V. M. Budnev, I. F. Ginzburg, G. V. Meledin and V. G. Serbo, Phys. Rept. **15**, 181 (1975).

Parametrizations of structure functions of proton

ALLM parametrization

- H. Abramowicz, E. M. Levin, A. Levy and U. Maor Phys. Lett. **B269**, (1991) 465

$$F_2(x, Q^2) = \frac{Q^2}{Q^2 + m_0^2}\left(F_2^{\mathcal{P}}(x, Q^2) + F_2^{\mathcal{R}}(x, Q^2)\right)$$

FFJLM parametrization

- R. Fiore, A. Flachi, L. L. Jenkovszky, A. I. Lengyel and V. K. Magas - Phys. Rev. **D70**, 054003 (2004)

$$\mathcal{I}m\alpha(s) = s^{\delta}\sum_n c_n \left(\frac{s - s_n}{s}\right)^{\mathcal{R}e\alpha(s_n)} \cdot \theta(s - s_n)$$

$$\mathcal{R}e\,\alpha(s) = \alpha(0) + \frac{s}{\pi} PV \int_0^{\infty} ds' \frac{\mathcal{I}m\alpha(s')}{s'(s' - s)}$$

Parametrizations of structure functions of proton

SU parametrization

- A. Szczurek, V. Uleshchenko
  Eur. Phys. J. **C12** (2000) 663-671

$$F_2^N(x, Q^2) = F_2^{N,VDM}(x, Q^2) + F_2^{N,part}(x, Q^2)$$

$$F_2^{N,VDM}(x, Q^2) = \frac{Q^2}{\pi} \sum_V \frac{M_V^4 \cdot \sigma_{VN}^{tot}(s^{1/2})}{\gamma_V^2 (Q^2 + M_V^2)^2} \cdot \Omega_V(x, Q^2)$$

$$F_2^{N,part}(x, Q^2) = \frac{Q^2}{Q^2 + Q_0^2} \cdot F_2^{asymp}(\bar{x}, \bar{Q}^2)$$

Describes higher twists at low Q^2

LUX-like structure function

- a newly constructed parametrization, which at $Q^2 > 9\,\mathrm{GeV}^2$ uses an NNLO calculation of F_2 and F_L from NNLO MSTW 2008 partons. It employs a useful code by the MSTW group to calculate structure functions. At $Q^2 < 9\,\mathrm{GeV}^2$ this fit uses the parametrization of Bosted and Christy in the resonance region, and a version of the ALLM fit published by the HERMES Collaboration for the continuum region. It also uses information on the longitudinal structure function from SLAC. As the fit is constructed closely following LUX QED work we call this fit LUX-like.

Arguments of structure functions

Calculated from photon transverse momentum and mass of the remnant.
Bjorken-x:

$$x_{Bj1} = \frac{Q_1^2}{Q_1^2 + M_X^2 - m_p^2} \,,$$

$$x_{Bj2} = \frac{Q_2^2}{Q_2^2 + M_Y^2 - m_p^2} \,.$$

Photon virtuality:

$$Q_1^2 \approx q_{1t}^2 \,,$$

$$Q_2^2 \approx q_{2t}^2 \,.$$

Forward proton

The ATLAS collaboration analysis impose the consistency requirements:

$$\xi_1 = \xi_{ll}^{+} \, , \; \xi_2 = \xi_{ll}^{-} \; . \tag{7}$$

The longitudinal momentum fractions of the photons were calculated in the ATLAS analysis as:

$$\begin{aligned} \xi_{ll}^{+} &= \left(M_{ll}/\sqrt{s}\right) \exp(+Y_{ll}) \; , \\ \xi_{ll}^{-} &= \left(M_{ll}/\sqrt{s}\right) \exp(-Y_{ll}) \; . \end{aligned} \tag{8}$$

Only lepton variables enter the formula. We will use the same formula in our analysis.

Integration parameters

Multiple integration (Vegas method):
$q_{1t}, q_{2t}, \phi_1, \phi_2, y_1, y_2, p_{t,diff}, \phi_{p_{t,diff}}$ and M_X or M_Y.

9 or 10 integration variables.
Many interesting correlations between variables.

Careful adjustment of ranges of some integration parameters is required.
$q_{1t}, q_{2t} <$ 100 - 500 GeV, $M_X, M_Y <$ 500 - 1000 GeV.

This depends on experimental cuts and acceptances.

Summary of our programs

We have 3 different versions of our codes:

- (a) calculate differential distributions using single unintegrated photon distributions
- (b) calculate differential distributions using doubly unintegrated photon distributions
- (c) generator version – generates unweighted events. Distributions done in an additional program or using Root program.

Results of the new analysis

In the calculations described below we shall take typical cuts on dileptons:

- -2.5 $< y_1, y_2 <$ 2.5
- $p_{1t}, p_{2t} >$ 15 GeV

We shall show also results with extra cuts on ξ_{ll}^{+} or ξ_{ll}^{-}.

In the following we do not exclude:

- mass window arround Z-boson mass m_Z, as was done in (ATLAS).
- cut on lepton acoplanarity

Double-elastic contribution

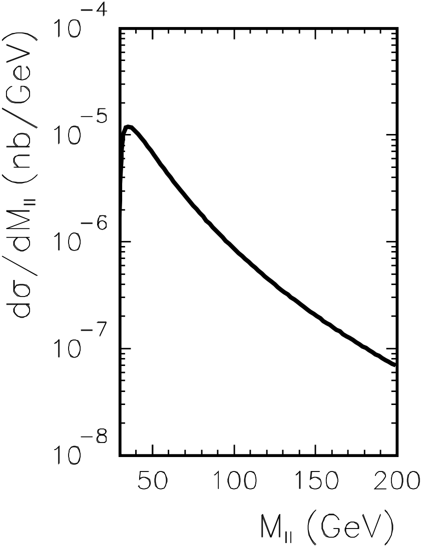

Double-elastic contribution

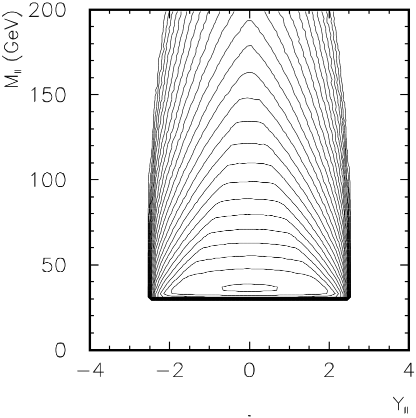

Rysunek: Here no cuts on neither ξ_1 nor ξ_2 were imposed.
The $p_{t,\mu} > 15$ GeV condition was imposed here.

Double-elastic contribution

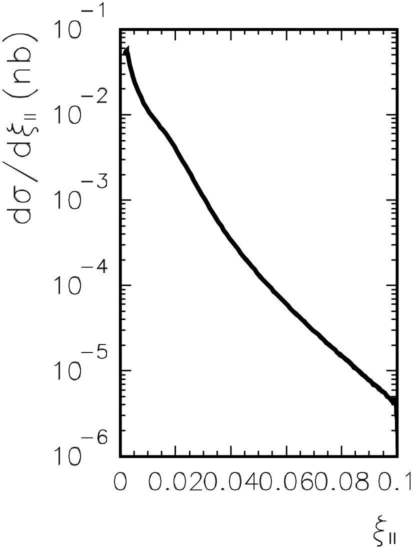

Double-elastic contribution

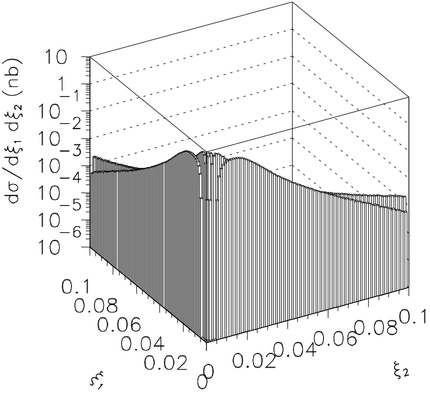

Rysunek: Two-dimensional distribution in $(\xi_{ll}^{+}, \xi_{ll}^{-})$ for the double-elastic mechanism.

Single-dissociative contribution

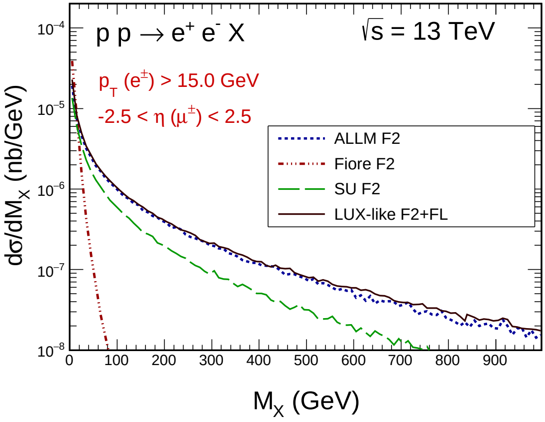

Rysunek: Distribution in the mass of the baryonic remnant system (M_X or M_Y) for different structure functions from the literature. In the case of SU parametrization only partonic contribution is included.

Single-dissociative contribution

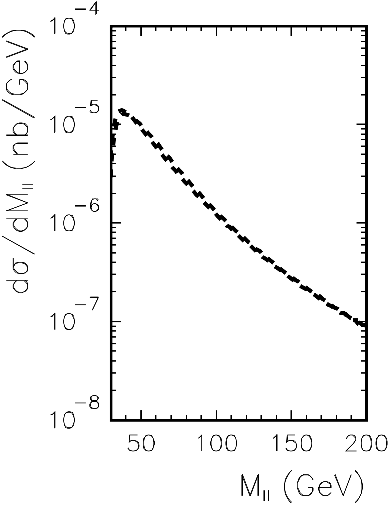

Rysunek: Distribution in dilepton invariant mass for

Single-dissociative contribution

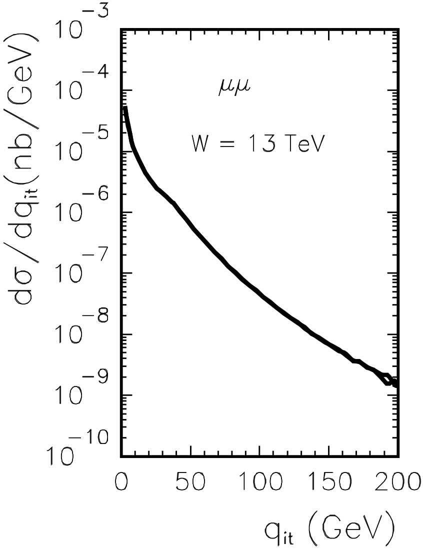

Single-dissociative contribution

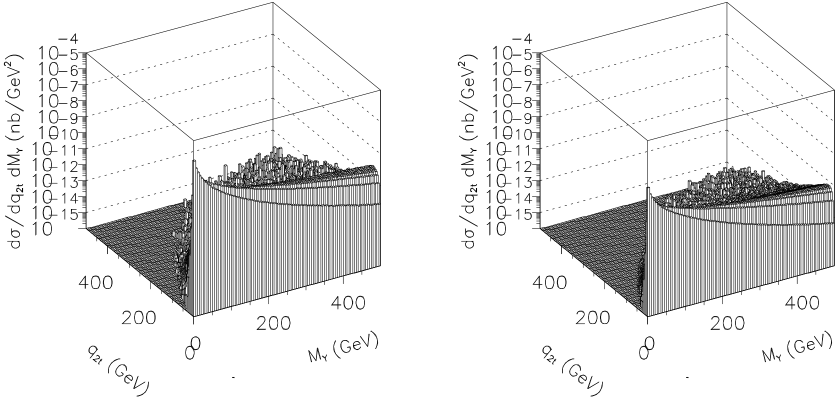

Rysunek: Two-dimensional distribution in (q_{2t}, M_Y) for elastic-inelastic contribution. We show results without ξ cut (left panel) and with ξ cut (right panel).

ξ_{ll}^{+} or ξ_{ll}^{-} cuts

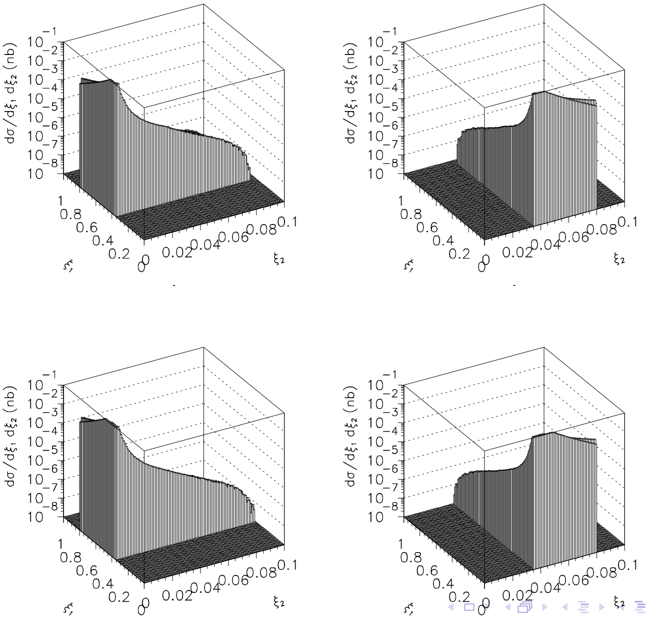

ξ_{ll}^{+} or ξ_{ll}^{-} cuts

Tablica: Integrated cross section for $\mu^+\mu^-$ with one p in 0.035 $< \xi_{ll}^{\pm} <$ 0.08. Here $p_{1t}, p_{2t} >$ 15 GeV and -2.5 $< y_1, y_2 <$ 2.5. In the paranthesis result with $p_{t,sum} <$ 5 GeV. 2UN – doubly unintegrated photon distribution and GEN – generator version.

contribution	c.s. in fb without ξ-cuts	c.s. in fb with ξ-cuts
elastic-elastic, cut on proton 1	358.68	5.4591
elastic-elastic, cut on proton 2	......	5.4592
elastic-inelastic, cut on proton 1, SU, 0-100 GeV	427.8949	10.0190 (3.3492)
inelastic-elastic, cut on proton 2 SU, 0-100 GeV	427.0130	10.0186 (3.3491)
elastic-inelastic, VDM (no Ω), 0-100 GeV	98.0215 (2UN)	
inelastic-elastic, VDM (no Ω), 0-100 GeV	98.0297 (2UN)	
elastic-inelastic SU partonic	449.1076 (2UN)	
inelastic-elastic SU partonic	449.0985 (2UN)	
elastic-inelastic, cut on proton 1, ALLM	468.6102 (2UN)	11.8292
inelastic-elastic, cut on proton 2, ALLM	468.6102 (2UN)	11.8294
elastic-inelastic, new Szczurek	461.5330 (2UN)	12.6046 [14.1823] (5.9311)
inelastic-elastic, new Szczurek	461.5750 (2UN)	12.6032 [14.1806] (5.9309)
elastic-inelastic, ALLM	571.871 (GEN)	9.711
inelastic-elastic, ALLM	571.562 (GEN)	9.621
elastic-inelastic, LUX-like, $F_2 + F_L$	635.215 (GEN)	19.894
inelastic-elastic, LUX-like, $F_2 + F_L$	635.102 (GEN)	19.831
elastic-inelastic, LUX-like, F_2 only	...... (GEN)	......
inelastic-elastic, LUX-like, F_2 only	656.702 (GEN)	......
elastic-inelastic, cut on proton 1, resonances	38.6709 (2UN)	0.57872
inelastic-elastic, cut on proton 2 resonances	38.6639 (2UN)	0.57872
elastic-inelastic, cut on proton 1, Δ^+	28.5844 (2UN)	0.42755
inelastic-elastic, cut on proton 2 Δ^+	28.5814 (2UN)	0.42763

ξ_{ll}^{+} or ξ_{ll}^{-} cuts

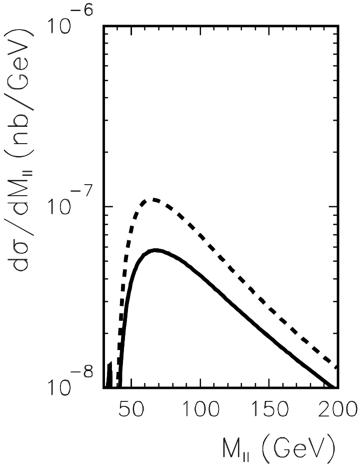

Rysunek: Distribution in dilepton invariant mass for four different contributions considered. The solid line is for double elastic contribution and the dashed line is for single dissociation contribution.

ξ-cut, double-elastic contribution

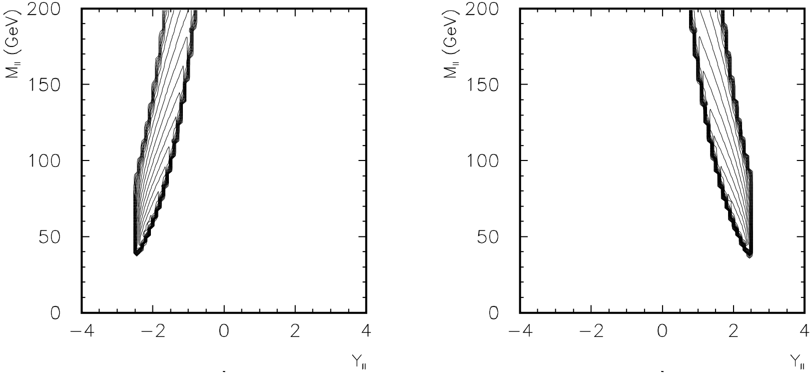

Rysunek: Here we have imposed experimental condition for ξ_2 (left panel) or ξ_1 (right panel).
The $p_{t,\mu} > 15$ GeV condition was imposed in addition.

ξ-cut, single-dissociative contribution

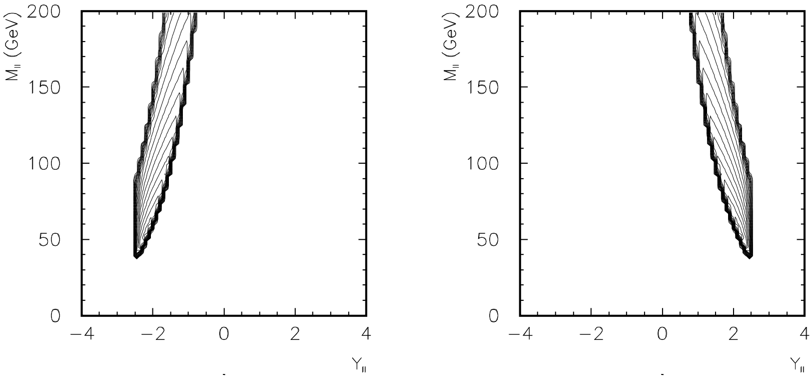

Rysunek: Here we have imposed experimental condition on ξ_1 (left panel) or ξ_2 (right panel).
Szczurek-Uleshchenko structure function parametrization was used.
The $p_{t,ll} > 15$ GeV condition has been imposed in addition.

ξ_{ll}^{+} or ξ_{ll}^{-} cuts

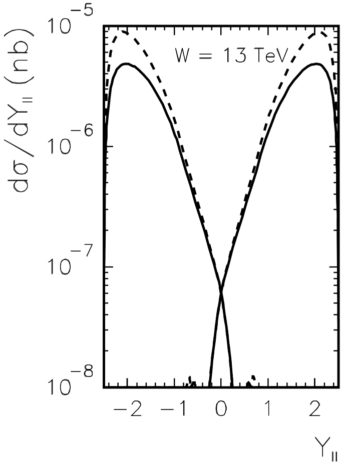

Rysunek: Here the cuts on ξ_{ll}^{+} or ξ_{ll}^{-} are imposed. The solid line is for double elastic contribution and the dashed line is for single dissociation contribution.

ξ_{ll}^{+} or ξ_{ll}^{-} cuts

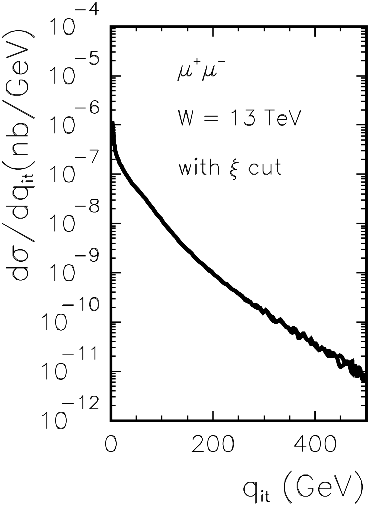

Rysunek: Distribution in q_{it}. Here the cuts on ξ_{ll}^{+} or ξ_{ll}^{-} are imposed.

ξ_{ll}^{+} or ξ_{ll}^{-} cuts

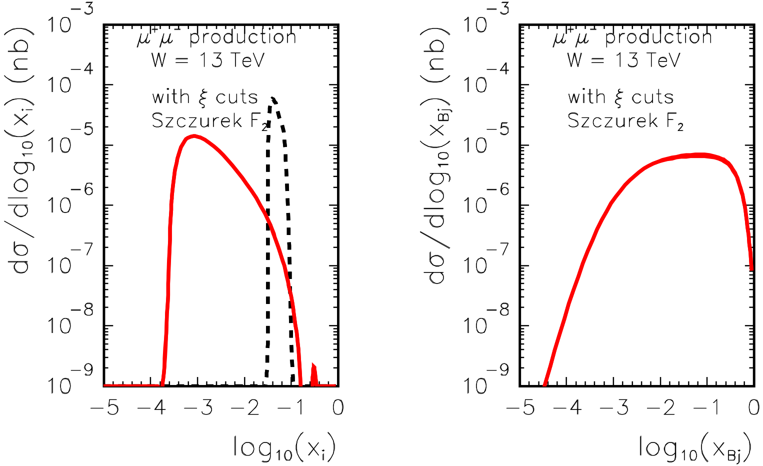

Arguments of the structure functions

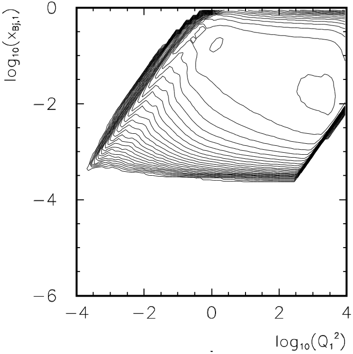

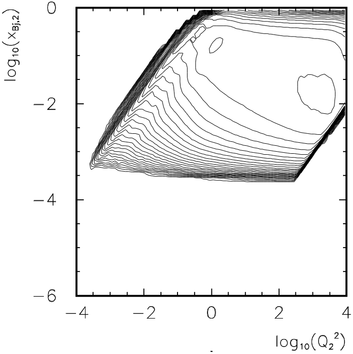

Both perturbative and nonperturbative regions

Arguments of the stucture functions, with $p_{t,pair}$ cut

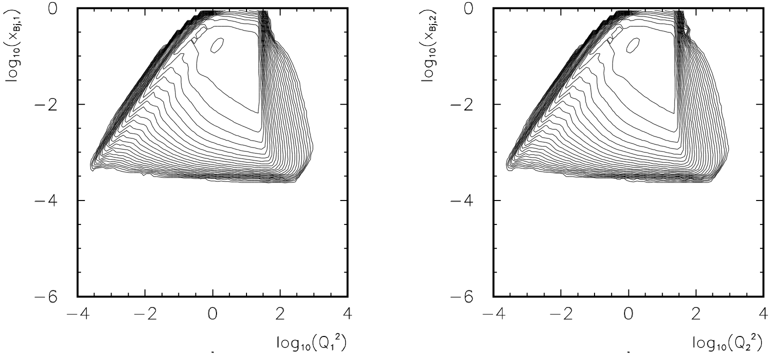

Big nonperturbative region – higher twists

ξ_{ll}^{+} or ξ_{ll}^{-} cuts

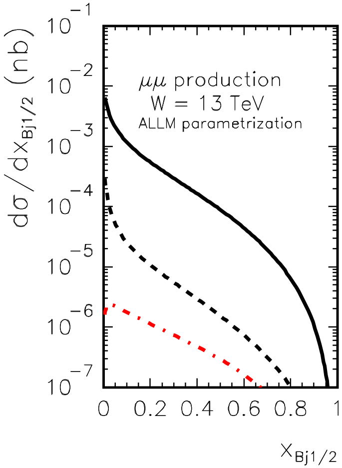

Rysunek: Distribution in x_{Bj} for single dissociative process. Shown are results without (solid line) and with (dashed line) cuts on longitudinal momentum fraction ξ.

In this calculation the ALLM parametrization of F_2 structure

ξ_{ll}^{+} or ξ_{ll}^{-} cuts

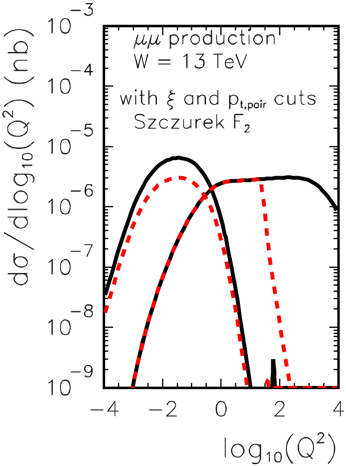

Rysunek: Distribution in $log_{10}(Q_i^2)$ for single dissociative process with cut on ξ and $p_{t,pair}$ (red dashed line). We show distributions for elastic (left) and inelastic (right) vertex.

In this calculation a new Szczurek parametrization of F_2 was used.

Effect of the cuts on acoplanarity

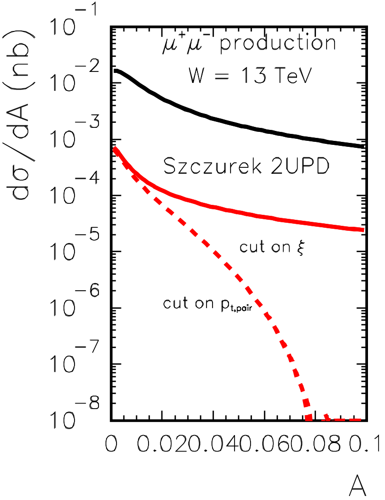

Rysunek: Acoplanarity distribution for SD contributions without any (upper black solid curve), with ξ cut (middle red solid curve) and with extra $p_{t,pair} < 5$ GeV condition (lower red dashed curve)

Minijets from DIS

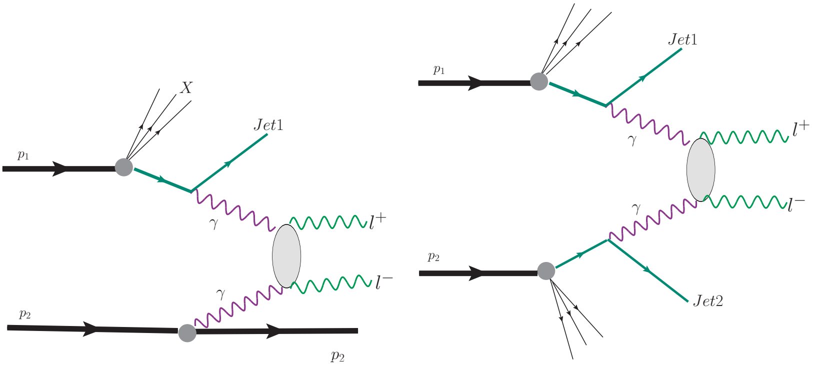

These are only leading-order diagrams

There could be also two-jet events (more difficult).

Remnant mass – y_{jet} correlations, with ξ cuts

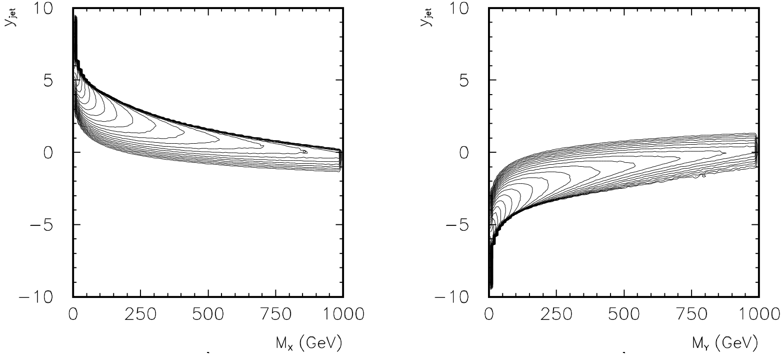

Rysunek: $M_X - y_{jet}$ and $M_Y - y_{jet}$ correlations.

Strong correlations

ξ_{ll}^{+} or ξ_{ll}^{-} cuts, minijets

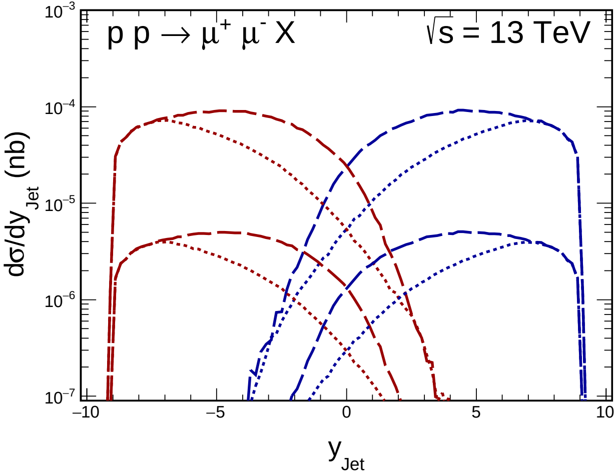

Rysunek: Distribution in rapidity of (mini)jets for inclusive case (upper curves) and for the case with cut on $\xi_{1/2}$. and $p_{t,pair} < 5$ GeV

SuperChic analysis

Tablica: Integrated cross section for $\mu^+\mu^-$ production in pb for $\sqrt{s}$ = 13 TeV using SuperChic program. $0.035 < \xi_{ll}^{\pm} < 0.08$. To calculate absorption effects we used model no 4 as implemented in the SuperChic generator.

reaction	no soft S_G	with soft S_G	$< S_G >$
-2.5 $< Y_{ll} <$ 2.5			
elastic-elastic	0.54438	0.50402	0.926
inelastic-elastic	0.89595	0.64283	0.717
elastic-inelastic	0.89587	0.64254	0.717
inelastic-inelastic	1.62859	0.24172	0.15
-2.5 $< y_1, y_2 <$ 2.5 in addition			
elastic-elastic	0.42268	0.39355	0.931
inelastic-elastic	0.69241	0.51092	0.738
elastic-inelastic	0.69246	0.51087	0.738
ξ cut in addition			
elastic-elastic, cut on ξ_1	0.00762	0.00675	0.886
elastic-elastic, cut on ξ_2	0.00762	0.00675	0.886
inelastic-elastic, cut on ξ_2	0.02718	0.01416	0.521
elastic-inelastic, cut on ξ_1	0.02717	0.01416	0.521
$p_{t,pair} <$ 5 GeV in addition			
elastic-elastic	....	....	.....
inelastic-elastic, cut on ξ_2	0.008035 (2000)	0.00435	0.541
elastic-inelastic, cut on ξ_1	0.008056 (2000)	0.00436	0.541

SuperChic analysis

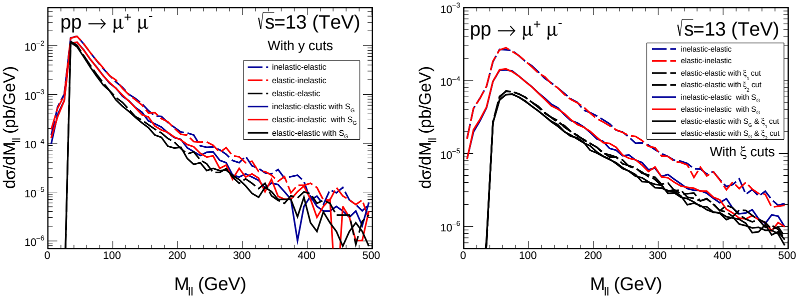

Rysunek: Distribution in dimuon invariant mass for the different contributions considered. We consider the case without ξ cuts (left panel) and with ξ cuts (right panel).

SuperChic analysis

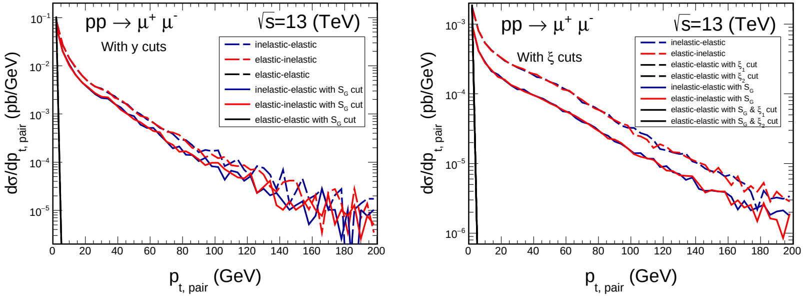

Rysunek: Distribution in dimuon transverse momentum for the different contributions considered. We consider the case without ξ cuts (left panel) and with ξ cuts (right panel).

SuperChic analysis, gap survival function

We shall show corresponding gap survival factor calculated as:

$$S_G(M_{ll}) = \frac{d\sigma/dM_{ll}|_{withSR}}{d\sigma/dM_{ll}|_{withoutSR}}, \quad (9)$$

$$S_G(p_{t,pair}) = \frac{d\sigma/dp_{t,pair}|_{withSR}}{d\sigma/dp_{t,pair}|_{withoutSR}}, \quad (10)$$

SuperChic analysis, gap survival function

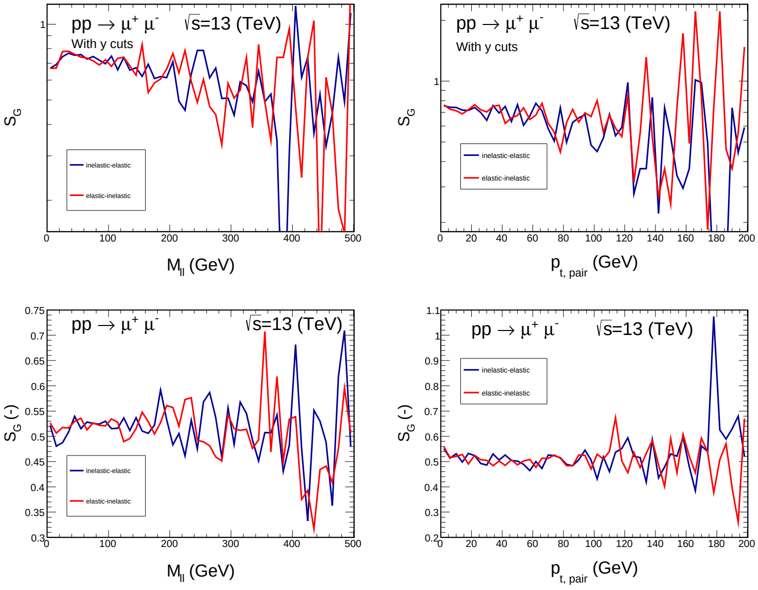

SuperChic analysis, gap survival function

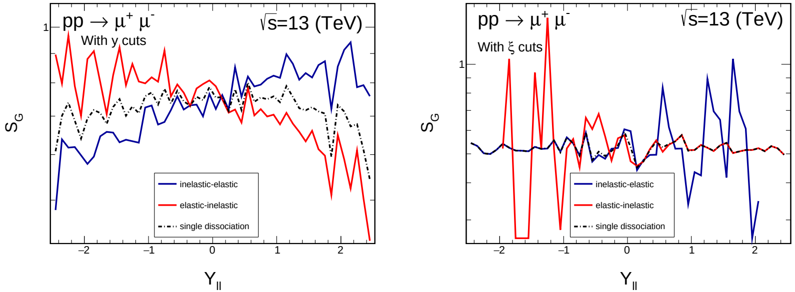

Rysunek: The soft gap survival factor as a function of rapidity of the $\mu^+\mu^-$ pair for single proton dissociation. We show the result without ξ cuts (left panel) and with ξ cuts (right panel). The dash-dotted black line is effective gap survival factor for both single-dissociation components added together.

SuperChic analysis, minijet

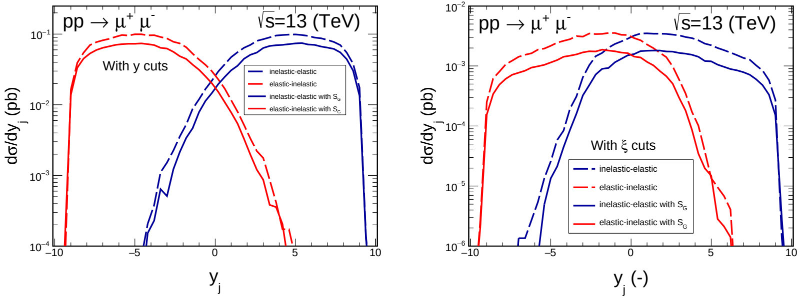

Rysunek: Distribution in the (mini)jet rapidity for the inclusive case of no ξ cut (left panel) and when the cut on ξ is imposed (right panel) for elastic-inelastic and inelastic-elastic contributions as obtained from the SuperChic generator We show result without (dashed line) and with (solid line) soft rescattering correction.

SuperChic, gap survival factor due to jet emission

Tablica: Gap survival factor due to minijet emission. In all cases $p_{1t}, p_{2t} > 15$ GeV.

contribution	without S_G	with S_G
cut on Y_{ll} only		
elastic-inelastic	0.76304	0.78756
inelastic-elastic	0.76278	0.78898
cut on y_1 and y_2 in addition		
elastic-inelastic	0.77366	0.79250
inelastic-elastic	0.76926	0.78744
cut on ξ_1 or ξ_2 in addition		
elastic-inelastic	0.48954	0.49986
inelastic-elastic	0.48374	0.49508
cut on $p_{t,pair} < 5$ GeV in addition		
elastic-inelastic	0.83462	(0.85600)
inelastic-elastic	0.83462	0.84960

Conclusions

- In the present paper we have discussed dilepton production via photon-photon fusion with one forward proton which can be measured in forward detectors such as AFP for the ATLAS experiment.
- We have consider both double-elastic and single-dissociative contributions (it was argued that the contribution of double dissociation is negligible when forward proton is measured).
- In the latter case we have considered both continuum production as well as Δ^+/resonance production. The continuum contribution is calculated for different parametrizations of the deep-inelastic structure functions from the literature.
- We have imposed conditions on ξ_1 or ξ_2 for the forward emitted protons. Several distributions have been shown and discussed.

Conclusions

- Particularly interesting is the distribution in M_{ll} and the distribution in Y_{ll} which has minimum at $Y_{ll} \sim 0$. The minimum at $Y_{ll} = 0$ is caused by the experimental condition on $\xi_{ll}^{\pm}$ related to the leading proton.
- We have also made calculations with the popular SuperChic generator and compared corresponding results to the results of our code(s). In general, the results are almost identical.
- We have calculated also soft rapidity gap survival factor as a function of M_{ll}, transverse momentum of the dilepton pair, mass of the proton remnant and Y_{ll}.
- No evident dependences on the variables for the single dissociation, except of distribution in Y_{ll}. We have found different (much larger) gap survival factor for fully elastic contribution than for single proton dissociation.

Conclusions

- The soft gap survival factor for single dissociative contribution strongly depends on whether proton is measured or not. It is significantly smaller when proton is measured.
- We have also calculated gap survival factor due to mini(jet) emission by checking whether the minijet enters or not the main detector.
- The second type of the gap survival (S_{jet}) also strongly depends on whether the outgoing proton is measured or not.
  It is about 0.8 for inclusive case (no proton measurement) and about 0.5 for the case with proton measurement in forward proton detector (with typical limited ξ value).
- small $p_{t,pair}$ $\rightarrow$ large y_{jet} $\rightarrow$ large S_{jet}.

Outlook

- In the moment only fiducial cross section was measured. In future one should measure differential distributions (better statistics, or lower $p_{l,t,min}$).
- Study large $p_{t,pair}$ region or even in bins of $p_{t,pair}$ and make a comparison bin-by-bin.
- When calculating absorptive corrections it is assumed that any interaction (independent of final state) will destroy rapidity gap or break another experimental condition on final state.
  This has no deep justification for experimental conditions implemented for large luminosities. (pile ups).
  Study theoretically final state related to absorptive proceses (extra pomeron exchange).
- So far only single jet topology is assumed.
  Single jet $\longrightarrow$ double jet production for calculating rapidity gap due to jets(s) emission.
- There are still missing mechanisms